Internal Medicine
The Japanese Society of Internal Medicine
doi: 10.2169/internalmedicine.7326-21
Intern Med 60: 3921-3926, 2021
http://internmed.jp

【 CASE REPORT 】

Possible Neoangiogenesis in Achilles Tendon Xanthoma with Familial Hypercholesterolemia: A Novel Approach to Achilles Tendon Xanthoma

Tetsu Tanaka[1], Kazuyuki Yahagi[1], Osamu Wada[2], Kai Ninomiya[1], Yu Horiuchi[1], Masahiko Asami[1], Hitomi Yuzawa[1], Kota Komiyama[1], Jun Tanaka[1], Jiro Aoki[1], Akitake Suzuki[3], Kazuho Ishizaki[2] and Kengo Tanabe[1]

Abstract:

Achilles tendon xanthoma (ATX) is one of the typical features of familial hypercholesterolemia (FH). The morphological evaluation of ATX by X-ray radiography is widely recognized; however, the utility of other imaging modalities remains unclear. We herein report two cases of FH in which Doppler ultrasound imaging demonstrated a microvascular flow in ATX that only rarely could be observed in normal Achilles tendons. Neoangiogenesis accompanies chronic inflammation and it may play an important role in the deposition of cholesterol crystals leading to ATX. In addition to the morphological evaluation of ATX, the assessment of neoangiogenesis may therefore be essential for the evaluation of ATX.

Key words: achilles tendon xanthoma, familial hypercholesterolemia, neoangiogenesis, ultrasonography, magnetic resonance imaging, superb micro-vascular imaging

(Intern Med 60: 3921-3926, 2021)
(DOI: 10.2169/internalmedicine.7326-21)

Introduction

Achilles tendon xanthoma (ATX) is one of the typical features of familial hypercholesterolemia (FH) and it is strongly associated with cardiovascular disease (1). The morphological assessment of the Achilles tendon using X-ray radiography is a widely recognized method to evaluate ATX in the diagnosis and risk classification of FH (2, 3). On the other hand, the mechanism underlying the development of ATX remains to be elucidated. Pathologically, chronic inflammation is indicated to be involved in the development of ATX (4, 5). The infiltration of macrophages and deposits of cholesterol crystals in ATX have been previously noted. However, the optimal clinical approach to the pathological changes in ATX has not yet been reported. As a result, we evaluated the pathological changes using ultrasonography (US) and magnetic resonance imaging (MRI) attributable to ATX. We herein describe two cases of FH with ATX in which the assessment of ATX by multimodality imaging was performed.

Case Reports

Case 1

A 51-year-old man without any prior medical history presented to our hospital with chest pain, and electrocardiography showed an elevation of ST-segmentation in leads V1 to V4. The patient was diagnosed to have ST-segmentation elevation acute myocardial infarction and therefore underwent emergent coronary angiography (CAG). CAG revealed a total occlusion of the proximal left anterior descending artery, and subsequent percutaneous coronary intervention (PCI) was performed with drug eluting stents. The patient had a high low-density lipoprotein (LDL) cholesterol level (181

[1]Division of Cardiology, Mitsui Memorial Hospital, Japan, [2]Division of Physiological Laboratory, Mitsui Memorial Hospital, Japan and [3]Division of Rheumatology, Mitsui Memorial Hospital, Japan
Received: February 13, 2021; Accepted: May 1, 2021; Advance Publication by J-STAGE: June 12, 2021
Correspondence to Dr. Kazuyuki Yahagi, yyahakazu@gmail.com

mg/dL) and a small dense LDL cholesterol level (87.2 mg/dL) without any lipid-lowering therapies. Additionally, X-ray radiography showed thickened bilateral Achilles tendon (Right; 11 mm, Left; 11 mm) (Fig. 1A). The patient did not have any familial histories of premature cardiovascular diseases and hypercholesterolemia. According to the Dutch Lipid Network Criteria (DLNC) for the diagnosis of FH (1), the patient was diagnosed with clinically definite FH.

Further assessment for the ATX with multimodality imaging, including US and magnetic resonance imaging(MRI) was performed. MRI, including T1-weighted image (T1WI) and T2-weighted image with 3-point Dixon technique, was obtained as previously reported (6). Sagittal T1WI showed an enlargement of the Achilles tendon (Fig. 1B). Additionally, an axial Dixon water image showed speckled high signal intensity in the Achilles tendon, whereas intermediate signal on T1WI and Dixon in-phase image and low signal on Dixon fat image were demonstrated (Fig. 1C-F). It was conceivable that the findings indicated an increase in fluid content in ATX. Notably, Superb Micro-Vascular Imaging (SMI) (Cannon Medical Systems, Tochigi, Japan), an ultrasound imaging technique to enable the visualization of microvascular flow signal, and power Doppler imaging (PDI) demonstrated a pulsative microvascular flow in the ATX (Fig. 2C-F). Such a microvascular flow signal has only rarely been observed in normal Achilles tendons (Fig. 2G, H).

According to current guidelines (7), high-intensity statin therapy was started, but the patient refused the administration of proprotein convertase subtilisin/kexin type 9 (PCSK 9) inhibitors.

Case 2

A 49-year man who underwent emergent PCI for acute myocardial infarction was diagnosed with clinically probable FH by DLNC because of premature coronary artery disease and bilateral Achilles tendon thickness (right: 10 mm, left: 10 mm). The patient had been treated with statin therapy, and a high LDL cholesterol level was not observed on admission (LDL cholesterol: 110 mg/dL), and the LDL cholesterol level before the statin therapy could not be confirmed. The patient had his microvascular flow assessed by SMI in the Achilles tendon xanthoma with high signal intensity on the Dixon water MR image (Fig. 3); however, PDI was not able to demonstrate the microvascular flow.

The patient started high-intensity statin therapy and was carefully followed after discharge.

Discussion

The assessment of ATX is clinically important in patients with prior histories of cardiovascular disease, especially acute coronary syndromes (ACS). Recent reports showed that the prevalence of ATX was higher in patients with ACS than in the general population (8-10). Additionally, ATX is strongly associated with a high risk of cardiovascular events and an impaired clinical outcome (11, 12), and, therefore, it is valuable to identify ATX among patients with cardiovascular disease for risk-stratification and management. In contrast, the underdiagnosis of FH still remains a major problem that must be addressed (13). X-ray radiography has been widely used for the measurement of Achilles tendon thickness in Japan; however, it is also important to examine the utility of other imaging tools for the assessment of ATX to improve the diagnostic accuracy.

The utility of other imaging modalities, including US and MRI, for the assessment of ATX has been recently reported (14-16). The Achilles tendon thickness assessed by US has a good relationship with the thickness assessed by X-radiograph and it can predict the development of asymptomatic atherosclerosis in coronary and carotid arteries (15, 17). Thus, the morphological assessment of the Achilles tendon by US or MRI has attracted attention as not only a diagnostic tool, but also as a risk-stratification tool for ATX.

Inflammatory reaction with the accumulation of extracellular lipid has been reported to be associated with the development of ATX (4, 5). Neoangiogenesis accompanies chronic inflammation and may play an important role in the deposition of cholesterol crystals within the Achilles tendon, which leads to glycosaminoglycan accumulation, chronic tendon degeneration, and xanthoma formation. Griffith et al. showed an elevation in signal intensity in ATX on the Dixon-water images that indicated an increase in the water content of the Achilles tendon (6), which was in line with the findings in our two cases. The increase in water content of ATX might be attributed in part to neoangiogenesis. In contrast, the ultrasonographic assessment for the pathological features in ATX has not been previously reported.

We experienced two patients in which the microvascular flow was observed in ATX by Doppler ultrasound imaging. The microvascular flow could indicate the presence of neoangiogenesis in ATX, which was supported by the high signal intensity on Dixon water images. To the best of our knowledge, this is the first report of neoangiogenesis in ATX with FH assessed by US. Neoangiogenesis in the Achilles tendon can also be identified by US in Achilles tendinopathy accompanying acute and high-grade inflammation (18, 19), but the two patients in this report had neither any symptoms of Achilles tendinopathy, including pain, nor a prior history of Achilles tendon injuries. Furthermore, the MR images were different from those in Achilles tendinopathy.

For the assessment of the neoangiogenesis, two Doppler ultrasound techniques were used. PDI is a conventional Doppler technique for the assessment of the microvascular flow; however, it is difficult to detect low-velocity blood flow signals in the tissue. SMI is a novel ultrasound imaging technique that was developed to overcome the limitations of conventional Doppler ultrasound which enables the visualization of neovascularization without the use of intravenous contrast. The utility of SMI has been proved for

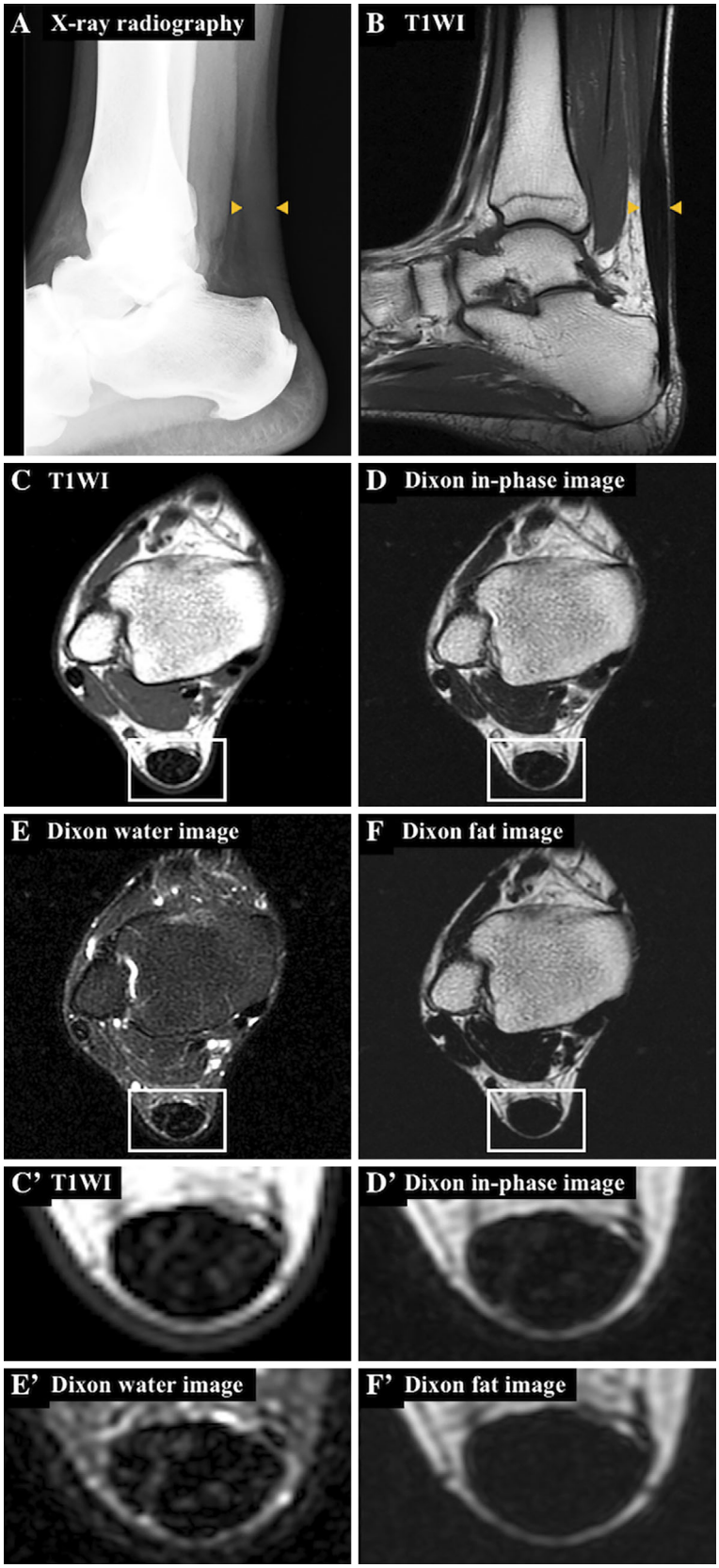

Figure 1. **X-ray radiography and magnetic resonance (MR) images for Case 1. A: Sagittal X-ray radiography shows an enlarged Achilles tendon (arrowhead). B: Sagittal T1-weighted MR image (arrowhead indicates Achilles tendon). C, C': Axial T1-weighted MR image at level of arrowheads shows intermediate signal intensity in Achilles tendon. D, D': Axial Dixon in-phase MR image shows intermediate signal intensity in Achilles tendon. E, E': Axial Dixon water MR image demonstrates high signal intensity in Achilles tendon. F, F': Axial Dixon fat MR image shows low signal intensity. T1WI: T1-weighted image**

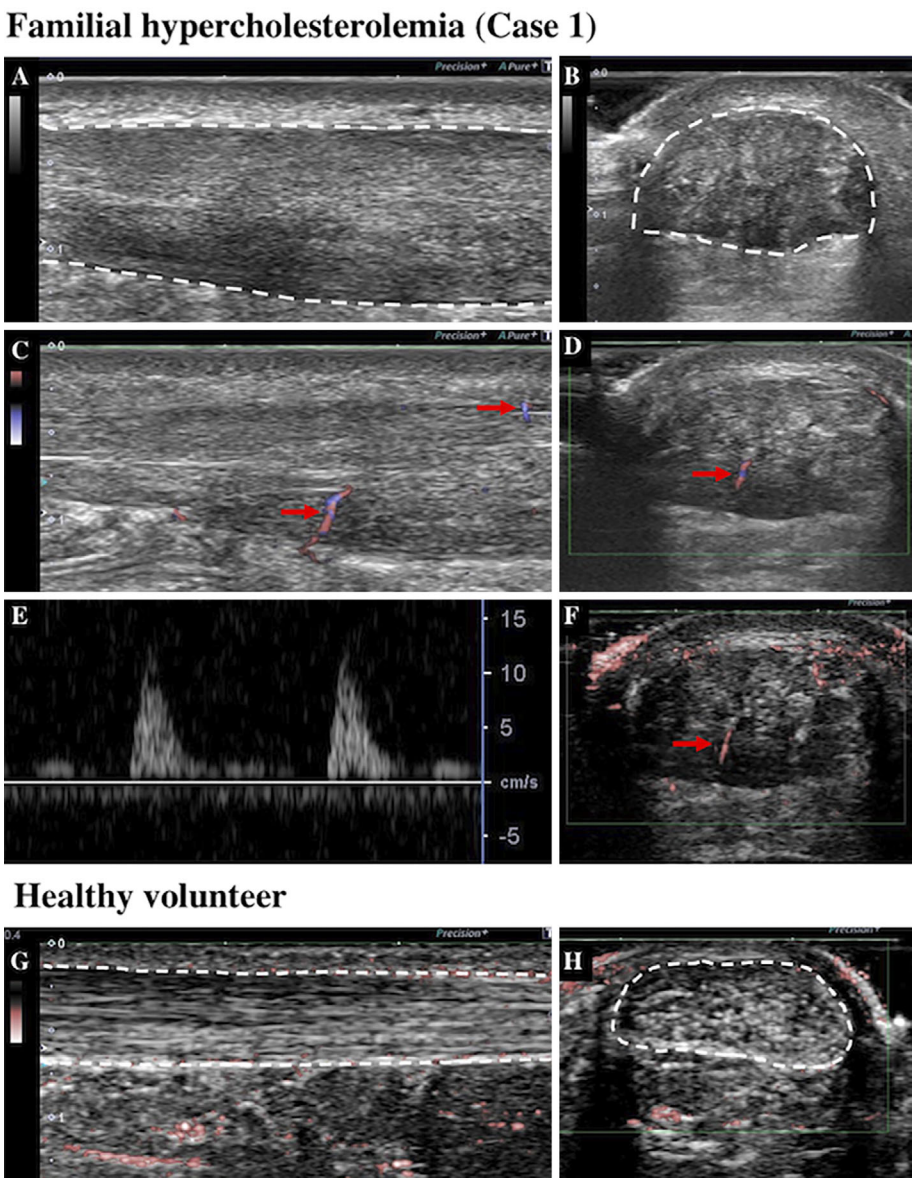

Figure 2. **Ultrasonographic images for Case 1 and a healthy volunteer. A: Long-axis 2-dimentional (2D) ultrasonographic (US) image. B: Short-axis 2D US image. C, D: Power Doppler imaging in long- and short-axis view (arrow indicates microvascular flow from both superficial and deep sides into Achilles tendon xanthoma). E: Power Doppler waveform. F: Superb Micro-Vascular Imaging (SMI) in short-axis view. G, H: SMI in long- and short-axis view in a healthy volunteer.**

evaluations of intra-plaque neoangiogenesis in carotid artery plaque and the activity of rheumatoid arthritis (20, 21). The microvascular flow signal in case 1 was observed by both SMI and PDI, whereas the microvascular flow signal in case 2 was only seen by SMI. Considering the detective sensitivities for the blood flow signal of SMI and PDI, the flow velocity of neoangiogenesis might have been lower in case 2 than in case 1.

Currently, the ultrasonographic assessment of ATX has not yet been established. However, there has recently been a growing interest in the assessment by US in Japan. Michikura et al. reported the optimal cut-off value of Achilles tendon thickness assessed by US for Japanese patients with FH (15). Therefore, the ultrasonographic measurements can be an essential part of the assessment of ATX in Japan. In addition, performing evaluations by Doppler ultrasound is simple and it has high reproducibility, although further investigations are still needed to examine its effectiveness in ATX. Thus, the Doppler ultrasound technique could be a useful assessment tool for ATX in addition to ultrasonographic morphological measurements.

In contrast, the assessment by multi-modality imaging has a disadvantage in the fact that there are some discrepancies in the values and normal ranges between the modalities. According to a previous study (15), the normal range of Achilles tendon thickness in US is lower than that in X-ray radiography. Compared to assessments by X-ray radiography, the Achilles tendon thickness assessed by US in our two cases was smaller, but still over the cut-off value of ATX in US (5.8 mm in men) (Case 1: 10 mm in US vs. 11 mm in

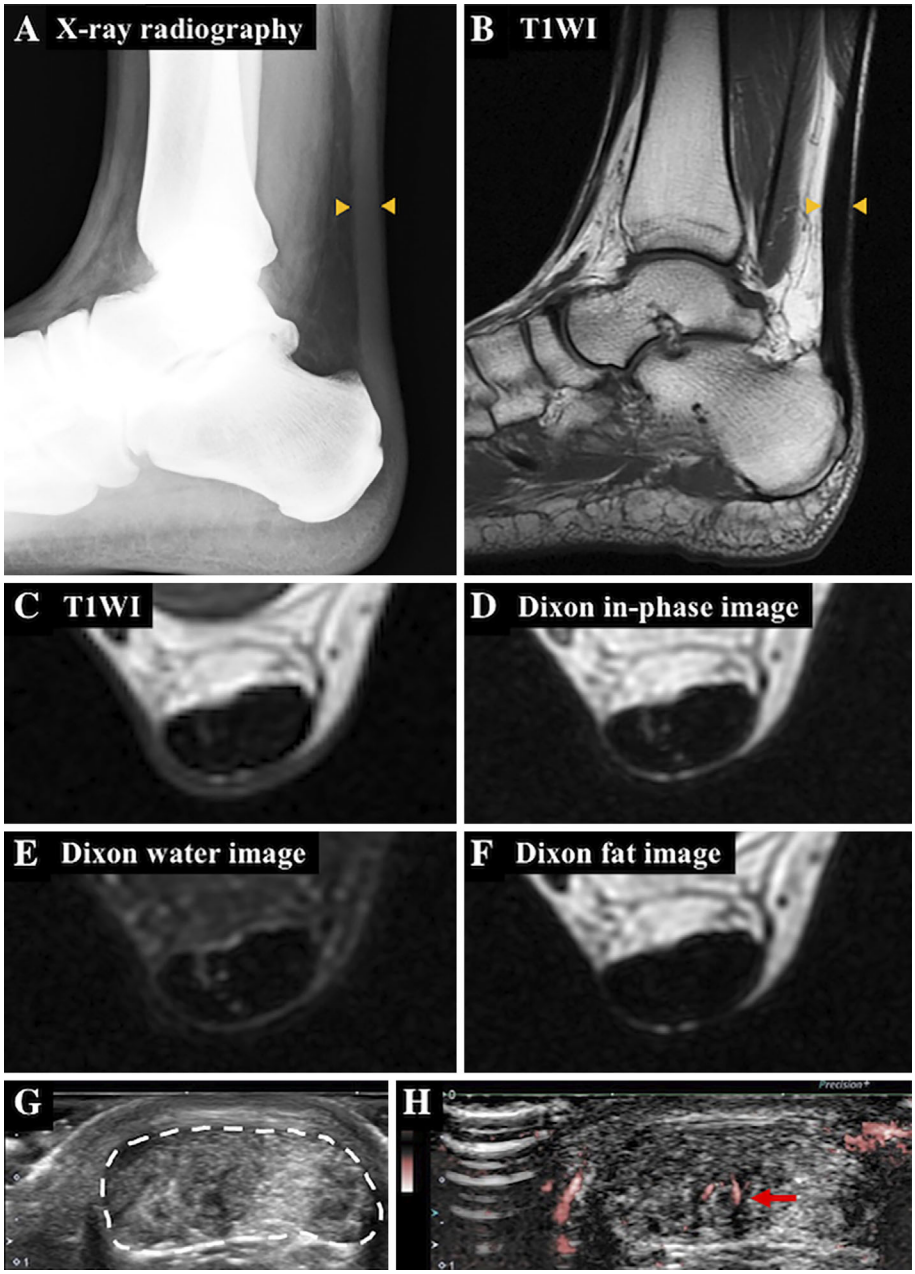

Figure 3. **X-ray radiography, magnetic resonance (MR) images, and ultrasonography for Case 2. A: Sagittal X-ray radiography shows an enlarged Achilles tendon (arrowhead). B: A sagittal T1-weighted MR image (the arrowhead indicates the Achilles tendon). C: An axial T1-weighted MR image at the level of the arrowheads shows intermediate signal intensity in the Achilles tendon. D: An axial Dixon in-phase MR image shows high signal intensity in the Achilles tendon. E: An axial Dixon water MR image demonstrates high signal intensity in the Achilles tendon. F: An axial Dixon fat image shows low signal intensity. G: A short-axis ultrasonographic image. H: Superb Micro-Vascular Imaging in the short-axis view. T1WI: T1-weighted image**

X-ray radiography; Case 2: 7.1 mm in US vs. 10.0 mm in X-ray radiography). In addition, the Achilles tendon thickness of the two cases assessed by MRI was 11.1 mm and 8.0 mm, respectively, although the normal range of MRI is still unclear. Therefore, the optimal cut-off value of Achilles tendon thickness as assessed by MRI still need to be investigated.

Our case report is associated with several limitations. First, we did not carry out any pathological validation of the microvascular flow as assessed by US. Second, since we reported a case series of two patients without any statistical analyses, the clinical impact of neoangiogenesis in ATX on cardiovascular disease and the prevalence of neoangiogenesis in patients with FH are still unclear. Therefore, further investigation with a larger number of patients and histological evaluations are called for to reveal the pathophysiology and clinical impact of neoangiogenesis in ATX.

Conclusion

We experienced two cases in which the microvascular flow, possibly indicating neoangiogenesis, in ATX was observed using a novel Doppler ultrasound technique. The findings of the present report may therefore lead to improvements in the evaluation of ATX and the management of patients with FH.

Author's disclosure of potential Conflicts of Interest (COI).
Kazuho Ishizaki: Honoraria, Canon Medical Systems. Kengo Tanabe: Honoraria, Canon Medical Systems, Philips, General Electric, Amgen and Sanofi.

References

1. Defesche JC, Gidding SS, Harada-Shiba M, Hegele RA, Santos RD, Wierzbicki AS. Familial hypercholesterolaemia. Nat Rev Dis Primers **3**: 17093, 2017.
2. Mangili LC, Miname MH, Silva PRS, et al. Achilles tendon xanthomas are associated with the presence and burden of subclinical coronary atherosclerosis in heterozygous familial hypercholesterolemia: a pilot study. Atherosclerosis **263**: 393-397, 2017.
3. Hashimoto T, Minami Y, Kakizaki R, et al. Achilles tendon thickening is associated with disease severity and plaque vulnerability in patients with coronary artery disease. J Clin Lipidol **13**: 194-200, 2019.
4. Yang Y, Lu H, Qu J. Tendon pathology in hypercholesterolaemia patients: epidemiology, pathogenesis and management. J Orthop Translat **16**: 14-22, 2019.
5. Abate M, Schiavone C, Salini V, Andia I. Occurrence of tendon pathologies in metabolic disorders. Rheumatology (Oxford) **52**: 599-608, 2013.
6. Griffith JF, Hu M, Yeung DKW, et al. Achilles tendon xanthomas: fat-water separation at baseline and after treatment. Radiology **285**: 876-884, 2017.
7. Kinoshita M, Yokote K, Arai H, et al. Japan Atherosclerosis Society (JAS) guidelines for prevention of atherosclerotic cardiovascular diseases 2017. J Atheroscler Thromb **25**: 846-984, 2018.
8. Harada-Shiba M, Ako J, Arai H, et al. Prevalence of familial hypercholesterolemia in patients with acute coronary syndrome in Japan: results of the EXPLORE-J study. Atherosclerosis **277**: 362-368, 2018.
9. Ohmura H, Fukushima Y, Mizuno A, et al. Estimated prevalence of heterozygous familial hypercholesterolemia in patients with acute coronary syndrome. Int Heart J **58**: 88-94, 2017.
10. Harada T, Inagaki-Tanimura K, Nagao M, et al. Frequency of Achilles tendon xanthoma in patients with acute coronary syndrome. J Atheroscler Thromb **24**: 949-953, 2017.
11. Hashimoto T, Minami Y, Asakura K, et al. Achilles tendon thickening is associated with higher incidence of adverse cardiovascular event in patients with coronary artery disease. Heart Vessels **36**: 163-169, 2021.
12. Oosterveer DM, Versmissen J, Yazdanpanah M, Hamza TH, Sijbrands EJ. Differences in characteristics and risk of cardiovascular disease in familial hypercholesterolemia patients with and without tendon xanthomas: a systematic review and meta-analysis. Atherosclerosis **207**: 311-317, 2009.
13. Nordestgaard BG, Chapman MJ, Humphries SE, et al. Familial hypercholesterolaemia is underdiagnosed and undertreated in the general population: guidance for clinicians to prevent coronary heart disease: consensus statement of the European Atherosclerosis Society. Eur Heart J **34**: 3478a-3490a, 2013.
14. Junyent M, Gilabert R, Zambon D, et al. The use of Achilles tendon sonography to distinguish familial hypercholesterolemia from other genetic dyslipidemias. Arterioscler Thromb Vasc Biol **25**: 2203-2208, 2005.
15. Michikura M, Ogura M, Yamamoto M, et al. Achilles tendon ultrasonography for diagnosis of familial hypercholesterolemia among Japanese subjects. Circ J **81**: 1879-1885, 2017.
16. Scott A, Zahradnik TM, Squier K, Beck C, Brunham LR. Diagnostic accuracy of ultrasound and MRI for Achilles tendon xanthoma in people with familial hypercholesterolemia: a systematic review. J Clin Lipidol **13**: 40-48, 2019.
17. Jarauta E, Junyent M, Gilabert R, et al. Sonographic evaluation of Achilles tendons and carotid atherosclerosis in familial hypercholesterolemia. Atherosclerosis **204**: 345-347, 2009.
18. Leung JL, Griffith JF. Sonography of chronic Achilles tendinopathy: a case-control study. J Clin Ultrasound **36**: 27-32, 2008.
19. Zanetti M, Metzdorf A, Kundert HP, et al. Achilles tendons: clinical relevance of neovascularization diagnosed with power Doppler US. Radiology **227**: 556-560, 2003.
20. Yu X, Li Z, Ren M, Xi J, Wu J, Ji Y. Superb microvascular imaging (SMI) for evaluating hand joint lesions in patients with rheumatoid arthritis in clinical remission. Rheumatol Int **38**: 1885-1890, 2018.
21. Zamani M, Skagen K, Scott H, Lindberg B, Russell D, Skjelland M. Carotid plaque neovascularization detected with superb microvascular imaging ultrasound without using contrast media. Stroke **50**: 3121-3127, 2019.